



**HAL**  
open science

## Non local approach for prediction of delamination onset

Pongsak Nimdum, Jacques Renard

► **To cite this version:**

Pongsak Nimdum, Jacques Renard. Non local approach for prediction of delamination onset. 18th international conference of composite materials, Aug 2011, Jeju, South Korea. 6 p. hal-00662221

**HAL Id: hal-00662221**

**<https://minesparis-psl.hal.science/hal-00662221>**

Submitted on 31 Jul 2018

**HAL** is a multi-disciplinary open access archive for the deposit and dissemination of scientific research documents, whether they are published or not. The documents may come from teaching and research institutions in France or abroad, or from public or private research centers.

L'archive ouverte pluridisciplinaire **HAL**, est destinée au dépôt et à la diffusion de documents scientifiques de niveau recherche, publiés ou non, émanant des établissements d'enseignement et de recherche français ou étrangers, des laboratoires publics ou privés.

# NON LOCAL APPROACH FOR PREDICTION OF DELAMINATION ONSET

P. Nimdum<sup>1\*</sup>, J. Renard<sup>1\*</sup>

<sup>1</sup> Mines-Paris Tech, CNRS UMR 7633, BP 87, F-91003 Evry, Cedex

\* Corresponding authors ([pongsak.nimdum@ensmp.fr](mailto:pongsak.nimdum@ensmp.fr), [jacques.renard@ensmp.fr](mailto:jacques.renard@ensmp.fr))

**Keywords:** *Thick composite, Criterion, Delamination, Interlaminar stresses*

## Abstract

The objective in this study is to predict initiation of delamination in epoxy reinforced carbon fiber of 2/2 twill weave fabric composites laminates during static testing. First, Micromechanical three-dimensional finite element models of the twill weave woven fabric are proposed to calculate ply equivalent behaviour using homogenous process. Then, we shall propose a criterion for onset of delamination under static loading. This criterion is based on average values of the components of the stress field and the law of Coulomb describing the friction between two bodies following assumptions: (i) a normal negative strength (compression) delays the delamination onset in shear (modes II and III); (ii) on the contrary, a positive normal stress accelerate the delamination onset and (iii) a normal negative strength is shear equal zero, cannot provoke the delamination onset. Identification of the different parameters of this criterion has been made with experimental Edge Delamination Tests (EDT). Validation was made with tensile tests performed on angle-ply textile laminates with drilled circular hole. Further numerical predictions are in good agreement with experimental results.

## 1. Introduction

Thick composite laminated structures able to support significant efforts, are more and more used for engineering structural parts. Then it is necessary to consider the ability of such laminates to resist from damage development, the consequence of which is mechanical degradation of properties (stiffness decrease). Thus, it requires appropriate design tools to prevent from damage evolution and predict the influence of damage on mechanical properties.

Damage mechanisms up to failure are rather complex in composites laminates. One reason is that several damage phenomena (matrix cracking,

delamination, fiber breaking, fiber/matrix interface debonding ...) are acting alone or coupled. This study is mainly focused on inter-ply delamination which could be more critical for structural parts and then has definitely to be avoided.

However, the application of unidirectional composites has several drawbacks such as impact resistance and tolerance in presence of a delamination. Therefore, the trend for composites applications is undergoing a transition towards the use of textile composite, also known as "woven fabric composites". These materials present various attractive [1-3] since it provides improved impact resistance, better in out-of-plane mechanical properties and improved damage tolerant in the presence of the delamination due to the non-planar interply structure of woven fabric composites. Nevertheless, the stiffness and strength behaviour of woven fabric composites are dependent on many parameters such as the characteristics of fibers and matrix and weave architecture [4] (weave type, packing density of yarns, undulation angle etc.).

Interlaminar normal and shear stresses can make edge delamination to appear, even up to laminate's failure. An efficient method for predicting delamination onset is thus needed. Two basic methods may be used for the delamination onset prediction: the stress method or the energy release rate one. Stress method requires interlaminar stresses to be determined at each interface and then to be compared with the material's strength characteristics. However, this method usually requires the help of the finite element method with fine meshing and supposes some specific ability. Most of stress criteria are expressed with average interlaminar stress [5-7] and the influence of a compressive stress stress is assumed to be negligible [6-7]. Lagunegrand et al. [8] shown that the compression should delay the delamination onset.

The objective in this study is to predict initiation of delamination in epoxy reinforced carbon fiber of 2/2

twill weave fabric composites laminates during static testing.

## 2. Experimental procedure

### 2.1 Material

The composite material of this study was carried out on carbon (T800)/epoxy composite material. The carbon fiber density was  $12.81 \text{ g/cm}^3$ . This study focuses on woven fabrics composites which the interlacing of the fill and warp yarns was formed according to the 2/2 twill weave pattern. The presence of weave structure induces very specific physical phenomena. We study on woven angle-ply laminates  $(0^\circ, \pm 20^\circ)_s$ ,  $(0^\circ, \pm 30^\circ)_s$  and  $(-30^\circ, -10^\circ, -50^\circ)_s$  with  $n = 1$  and 2. One ply thickness is 0.65 mm and the fiber volume fraction is  $V_f = 52.9\%$ .

### 2.2 Experimental procedure

All specimens were cut from plates using the diamond wheel saw and were bonded with glass/epoxy or aluminium tabs onto each specimen end. During tensile tests, the specimen surface (length 65 mm) is recorded at different loading with a digital CCD camera under white light illumination.

## 3. Experimental result

### 3.1 Damage mechanism on angle-ply

In generally, due to edge effect lead to free-edge stress singularity at interface of adjacent layers and result in the onset of delamination, also called interlaminar delamination. Fig. 1 illustrate the onset delamination at interface  $+20^\circ_n / -20^\circ_n$  and  $-10^\circ_n / -50^\circ_n$ . These delaminations are not straight (plan) but bended. They propagate to follow the interface of adjacent yarns and the crimp yarns. These delaminations are considered as shear mode (mode II and III) for the first and the second one but as a mixed-mode for the last one, respectively. Table 1 shown the experimental result of onset of delaminates at free edge in angle-ply.

After the interlaminar delamination appeared, we investigate on stiffness degradation and find that the modulus decrease can be divided into three stages: (i) initial region with a slightly decrease stiffness reduction of about 2% - 4%, and then, (ii) a rapid decrease of stiffness (about 10%), and finally

become unstable and lead to the final failure of specimen.

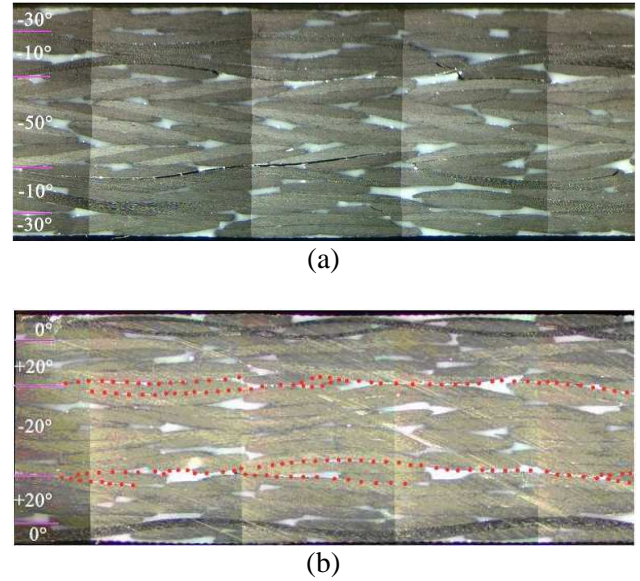


Fig.1. (a) Mixed-mode and (b) open-mode delamination during static loading.

Table 1

Experiment result on angle-ply laminates

| Laminate                                  | Interface of delamination   | $\sigma_{onset}^{Experiment}$ (MPa) |
|---|-----------------------------|-------------------------------------|
| $(0^\circ, \pm 20^\circ)_s$               | $+20^\circ / -20^\circ$     | 425-450                             |
| $(0^\circ_2, \pm 20^\circ_2)_s$           | $+20^\circ_2 / -20^\circ_2$ | 312.5-337.5                         |
| $(0^\circ, \pm 30^\circ)_s$               | $+30^\circ / -30^\circ$     | 405-430                             |
| $(0^\circ_2, \pm 30^\circ_2)_s$           | $+30^\circ_2 / -30^\circ_2$ | 287.5-321.5                         |
| $(-30^\circ, -10^\circ, -50^\circ)_s$     | $-10^\circ / -50^\circ$     | 270-295                             |
| $(-30^\circ, -10^\circ_2, -50^\circ_2)_s$ | $-10^\circ_2 / -50^\circ_2$ | 265-290                             |

## 4. FEM analysis

### 4.1 Homogeneous procedure

In order to take place heterogeneous woven ply by equivalent homogenous ply, a homogenization procedure in the twill-weave unit cell ( $9.2 \times 9.2 \text{ mm}$ ) (Fig. 2) is used in this study. First, 3D finite element taken into account the effects of yarns interlacing and orientation of adjacent layers. The mechanical response of a yarn is determined and validated by tensile tests. The yarn (straight region) was assumed transversely isotropic and linear elastic and is given in Table 2, while the property of the epoxy matrix is

isotropic elastic with Young's modulus equal to 3.1 GPa and Poisson's ratio equal to 0.39.

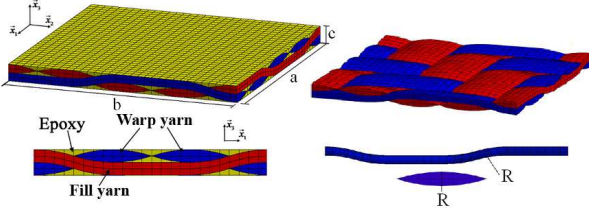


Fig.2. 3D finite element mesh

To determine the global mechanical properties, the periodic boundary conditions in  $\bar{x}_1 - \bar{x}_2$  direction were applied. We assume small deformation assumption, therefore the volume variation is quietly small. The microscopic stress  $\tilde{\Sigma}_{ij}$  and strain  $\tilde{E}_{ij}$  tensors must be the averages of the microscopic corresponding quantities (see in Eq.(1)). The mechanical properties of equivalent homogenous ply were determined after a homogeneous procedure as detail in table 3.

$$\begin{cases} \text{div } \tilde{\sigma} = 0 \\ \tilde{\sigma} = \tilde{c} : \tilde{\varepsilon} & \text{on } \Omega \\ \tilde{u} = \tilde{E} \cdot \tilde{x} + \tilde{v} & \text{with } \tilde{v} \text{ } \bar{x}_1 - \bar{x}_2 \text{ periodic} \\ \tilde{u} = \tilde{E} \cdot \tilde{x} \text{ or } \tilde{t} = \tilde{\Sigma} \cdot \tilde{n} & \text{on } \partial\Omega \text{ in } \bar{x}_3 \text{ direction} \\ \tilde{\sigma} \cdot \tilde{n} & \bar{x}_1 - \bar{x}_2 \text{ anti - periodic on } \partial\Omega \\ \langle \tilde{\sigma} \rangle = \langle \tilde{\Sigma} \rangle \text{ or } \langle \tilde{\varepsilon} \rangle = \langle \tilde{E} \rangle \end{cases} \quad (1)$$

Table 2

Mechanical properties of a T800s fill/warp yarn

| $E_{11}$ (GPa) | $E_{22} = E_{33}$ (GPa) | $G_{23}$ (GPa) | $G_{12} = G_{13}$ (GPa) | $\nu_{23}$ | $\nu_{12} = \nu_{13}$ |
|----------------|-------------------------|----------------|-------------------------|------------|-----------------------|
| 210.00         | 9.250                   | 3.7            | 4.7                     | 0.25       | 0.33                  |

Table 3

Equivalent homogeneous ply behaviour of fabric

| $E_{11} = E_{22}$ (GPa) | $E_{33}$ (GPa) | $G_{23} = G_{13}$ (GPa) | $G_{12}$ (GPa) | $\nu_{23} = \nu_{13}$ | $\nu_{12}$ |
|-------------------------|----------------|-------------------------|----------------|-----------------------|------------|
| 60.53                   | 7.795          | 2.685                   | 3.231          | 0.489                 | 0.0336     |

In order to study the delamination onset in angle-ply laminate, therefore, the 3D finite element model of equivalent homogenous ply can be used. The mesh near the interface corner of free-edge is refined in

order to represent the stresses singularity due to the free-edge effect.

## 4.2 Delamination onset

### 4.2.1 Delamination onset criterion

This criterion is based on the law of Coulomb describing the friction between two bodies following assumptions: (i) a normal negative strength (compression) delays the delamination onset in shear (modes II and III); (ii) on the contrary, a positive normal stress accelerate the delamination onset and (iii) a normal negative strength is shear equal zero, cannot provoke the delamination onset (Eq.(1)). We note that in this study, we assume that two modes of the interlaminar shear strength are similar.

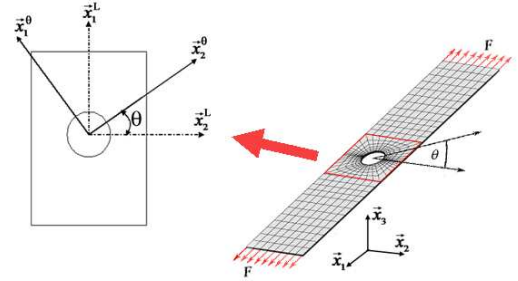


Fig.3. Circular-hole specimen

In order to apply this criterion in Eq.(2) to circular-hole specimens, the interlaminar tensile and shear strengths are modified. The transformation of coordinates as a function of angle of  $\theta$  is used (Fig. 3.) The delamination onset criterion to circular-hole specimens is therefore shown in Eq.(3).

$$\begin{aligned} & \frac{\langle F_3 \rangle^+{}^2}{Y_r^2} + \frac{\left( |F_1| + k_1 \langle F_3 \rangle^- \right)^2}{S_1^2} \\ & + \frac{\left( |F_2| + k_2 \langle F_3 \rangle^- \right)^2}{S_2^2} = 1 \end{aligned} \quad (2)$$

with

$$\vec{F} = \begin{Bmatrix} F_1 \\ F_2 \\ F_3 \end{Bmatrix} = \tilde{\sigma} \cdot \hat{r} = \begin{bmatrix} \sigma_{11} & \sigma_{12} & \sigma_{13} \\ \sigma_{12} & \sigma_{22} & \sigma_{23} \\ \sigma_{13} & \sigma_{23} & \sigma_{33} \end{bmatrix} \begin{Bmatrix} 0 \\ 0 \\ 1 \end{Bmatrix} = \begin{Bmatrix} \sigma_{13} \\ \sigma_{23} \\ \sigma_{33} \end{Bmatrix}$$

and

$$\langle x \rangle^+ = \begin{cases} x & \text{if } x > 0 \\ 0 & \text{if } x \leq 0 \end{cases}$$

$$\langle x \rangle^- = \begin{cases} 0 & \text{if } x > 0 \\ x & \text{if } x \leq 0 \end{cases}$$

Where  $Y_T$ ,  $S_1$  and  $S_2$  are interlaminar tensile strength (mode I), shear strength in mode II and III of interface, respectively  $k_1$  and  $k_1$  are friction coefficients between interface of material.

$$\begin{aligned} & \frac{\langle F_3 \rangle^+}{Y_T^2} + \frac{\langle F_3 \rangle^-}{S^2/(2k^2)} + \frac{|F_2| \langle F_3 \rangle^- (\cos \theta + \sin \theta)}{S^2/(2k)} \\ & + \frac{|F_1| \langle F_3 \rangle^- (\cos \theta - \sin \theta)}{S^2/(2k)} + \frac{(F_2)^2}{S^2} + \frac{(F_1)^2}{S^2} = 1 \end{aligned} \quad (3)$$

#### 4.2.2 Non local method

The edge effect generally leads to the stress singularities near free-edge interface which occur when we use the finite element analysis method. Consequently the use of local criterion, for delamination onset depends on the mesh size in the free-edge area. In order to avoid the mesh-dependent of finite element approximation, the delamination onset criterion should not only take account of point stress but also their distributions. As a result, many non-local stress criteria have been developed. The first category of criteria [5,7,9] is based on the average stress, often using an integral method, over an area or a line. In this study non-local stress criteria corresponding to the three anti-plane stresses which are defines as:

$$\bar{\sigma}_{ij}(y_0) = \frac{1}{y_0} \int_0^{y_0} \sigma_{ij}(\xi) d\xi \quad (4)$$

where  $\sigma_{ij}$  and  $\bar{\sigma}_{ij}$  represent three local and average anti-plane stresses at interface, respectively.  $y_0$  is the critical length over which three average stresses are determined.

Then, the second categories of criterions represented the gradient of stress singularities using the weight function which allow to evaluate the weight changes in quantities [10,11]. In this study, we have been selected based on the average stress and their gradients in the vicinity of singular point. The gradient effect is taken into account by the first order derivative. The non-local stresses are then defined in Eq.(5). However, due to the main aim of this paper, we will investigate the delamination onset at

interface of adjacent layers. As a result, we can suppose that the gradient effects have been only evaluated along the interface. The Eq. (5) can then be rewritten as Eq.(6).

$$\tilde{\sigma}_{ij} = \begin{cases} \sigma_{ij} & \text{if } y = 0 \\ \sigma_{ij} + h \cdot \left( \frac{\partial \sigma_{ij}}{\partial x} + \frac{\partial \sigma_{ij}}{\partial y} + \frac{\partial \sigma_{ij}}{\partial z} \right) & \text{if } y > 0 \end{cases} \quad (5)$$

where  $h$  is characteristic length for taking into account the gradient effect. Note that  $h$  depends on the constituents, their geometries (lamina, woven-fabrics) of composites studied.

To summarize that, the average non-local stresses ( $\bar{\tilde{\sigma}}_{ij}$ ) which take into the effect of gradient on a neighborhood are determined upon the critical length.

$$\bar{\tilde{\sigma}}_{ij} = \begin{cases} \sigma_{ij} & \text{if } y = 0 \\ \sigma_{ij} + h \cdot \frac{\partial \sigma_{ij}}{\partial y} & \text{if } y > 0 \end{cases} \quad (6)$$

#### 4.2.3 Identification of criterion parameters

In order to determine the all parameters of interest, the graphical method [9] with previous experimental results are used. The graphical method for assessment of criterion parameters of non local criteria without,  $\bar{\sigma}_{ij}$ , and with gradient adding,  $\bar{\tilde{\sigma}}_{ij}$  as shown in Fig. 4 are performed with various thickness and stacking sequences. The identification result is shown in Table 5.

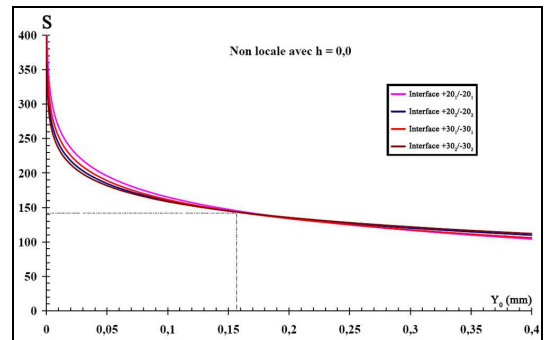


Fig.4. Graphical results method in average non local. We note that the interlaminar tensile strength of interface is relative low compare with interlaminar shear strength. However, this results is correlated

with previous study [9] and Arcan-Mines test. Furthermore, Table 6 shows a good agreement between experimental values and numerical prediction.

Table 5  
Identifications of parameters criterion results

| $h$  | $y_0$ | $k$  | $S$   | $Y_T$ |
|------|-------|------|-------|-------|
| 0.0  | 0.16  | 0.01 | 141.5 | 30.0  |
| 0.01 | 0.21  | 0.01 | 147.5 | 28.0  |
| 0.02 | 0.3   | 0.01 | 141.0 | 30.0  |
| 0.03 | 0.3   | 0.01 | 147.0 | 30.0  |

Table 6  
Stress prediction vs. experimental results on angle-ply laminate

| Laminate                                    | Interface of delamination   | $\sigma_{onset}^{Prediction}$ (MPa) |          |          |
|---|-----------------------------|-------------------------------------|----------|----------|
|   |                             | $h=0.0$                             | $h=0.01$ | $h=0.02$ |
| $(0^\circ, \pm 20^\circ)_s$                 | $+20^\circ / -20^\circ$     | 430                                 | 429      | 430      |
| $(0^\circ_2, \pm 20^\circ_2)_s$             | $+20^\circ_2 / -20^\circ_2$ | 323                                 | 324      | 325      |
| $(0^\circ, \pm 30^\circ)_s$                 | $+30^\circ / -30^\circ$     | 415                                 | 417      | 418      |
| $(0^\circ_2, \pm 30^\circ_2)_s$             | $+30^\circ_2 / -30^\circ_2$ | 288                                 | 291      | 290      |
| $(-30^\circ, -10^\circ, -50^\circ)_s$       | $-10^\circ / -50^\circ$     | 276                                 | 270      | 283      |
| $(-30^\circ_2, -10^\circ_2, -50^\circ_2)_s$ | $-10^\circ_2 / -50^\circ_2$ | 282                                 | 280      | 286      |

**5. Prediction of delamination onset in circular-hole specimens**

In order to validate in previous section for the delamination onset criterion, the experimental tests and numerical simulations in circular-hole specimens is used under tensile loading.

**5.1 Experimental procedure**

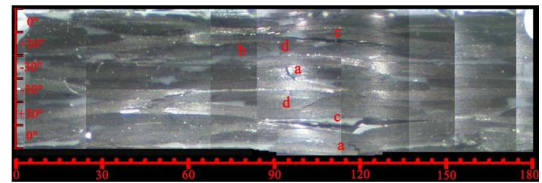
The specimen geometry for the open hole tensile test had a hole diameter ( $\phi$ ) of 10 mm, a length ( $L$ ) of 270 mm and a width ( $l$ ) of 30 mm. The loading-unloading of tensile testing for  $(0^\circ, \pm 20^\circ)_s$ ,  $(0^\circ, \pm 30^\circ)_s$ ,  $(0^\circ, \pm 30^\circ_2)_s$  and  $(0^\circ, \pm 20^\circ_2)_s$  were preformed. The circular hole specimens, polished prior to testing, are observed at different stress level with the mirror which allow its to rotate ( $\alpha$ ) around the axe. This angle is defined to respect the applied loading direction,  $\alpha = \theta + 90^\circ$

The experimental observations tensile test show that all specimens consist of three major damage (Fig. 6): intra-ply cracking (“a”), the intra-ply delamination (“b”) and finally inter-ply delamination (“c” and “d”). It should be underline that typical damage mode of delaminage at the interfaces  $+20^\circ / -20^\circ$

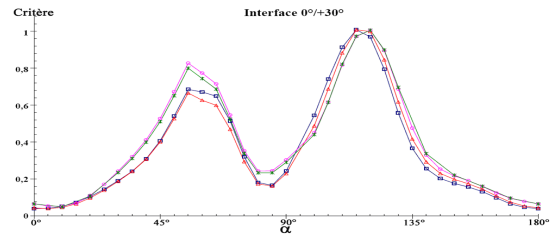
and  $+30^\circ / -30^\circ$  is more difficult to observe due to interlaminar shear mode (mode III). While, the interfaces  $0^\circ / +20^\circ$  and  $0^\circ / +30^\circ$ , the delamination occur as a mixed mode representing not only crack edge sliding but also crack edge opening. The open mode is generally easier to observe because delaminations propagation spontaneous.

**5.3 Delamination onset prediction: location and stress level**

In order to carry out the damage mechanisms at edge of circular hole, the finite element method with equivalent homogeneous ply has been use. The numerical results of all stacking sequences of a laminate composite show the good accuracy of location predictions to delamination onset compared with the experimental results (Table 6.), as example illustrate in Fig.8 for  $(0^\circ, \pm 30^\circ)_s$  laminate case. The two approaches criterion, with and without gradients, predict to the same location of delamination onset. The numerical results show also a good correlation in term of damage mode (I, II and III) with experimental results.



(a)



(b)

Fig.8. (a) Damage mechanisms in  $(0^\circ, \pm 30^\circ)_s$  laminate; (b) numerical prediction

For the prediction of delamination onset stress, there is a good correlation between the numerical results and experimental observations. The slight prediction error of  $+20^\circ / -20^\circ$  and  $+30^\circ / -30^\circ$  interfaces can be found (Table 7) due to a typical mode III of delamination onset. Consequently, this mode of

delamination onset is more difficult to observe due to the closing mode. To overcome this problem, high accuracy observation techniques like acoustic emission are necessary.

Table 6  
Numerical prediction vs. experimental result of position of delamination onset

| Interface of delamination     | Experiment | $\alpha(^{\circ})$ |          |          |
|-------------------------------|------------|--------------------|----------|----------|
|                               |            | $h=0.0$            | $h=0.01$ | $h=0.02$ |
| $0^{\circ}/+20^{\circ}$       | 90°-120°   | 110°               | 110°     | 110°     |
| $+20^{\circ}/-20^{\circ}$     | 85°-95°    | 90°                | 90°      | 90°      |
| $0^{\circ}_2/+20^{\circ}_2$   | 90°-120°   | 110°               | 110°     | 110°     |
| $+20^{\circ}_2/-20^{\circ}_2$ | 70°-90°    | 90°                | 90°      | 90°      |
| $0^{\circ}/+30^{\circ}$       | 90°-125°   | 115°               | 115°     | 115°     |
| $+30^{\circ}/-30^{\circ}$     | 85°-95°    | 90°                | 90°      | 90°      |
| $0^{\circ}_2/+30^{\circ}_2$   | 90°-130°   | 115°               | 115°     | 115°     |
| $+30^{\circ}_2/-30^{\circ}_2$ | 80°-95°    | 90°                | 90°      | 90°      |

Table 7  
Numerical prediction vs. experimental result of delamination onset stress

| Interface of delamination     | Experiment (MPa) | $\sigma_{onset}^{Prediction}$ (MPa) |          |          |
|-------------------------------|------------------|-------------------------------------|----------|----------|
|                               |                  | $h=0.0$                             | $h=0.01$ | $h=0.02$ |
| $0^{\circ}/+20^{\circ}$       | 300-350          | 346                                 | 355      | 434      |
| $+20^{\circ}/-20^{\circ}$     | 300-350          | 255                                 | 282      | 325      |
| $0^{\circ}_2/+20^{\circ}_2$   | 250-290          | 331                                 | 338      | 400      |
| $+20^{\circ}_2/-20^{\circ}_2$ | 250-290          | 208                                 | 226      | 261      |
| $0^{\circ}/+30^{\circ}$       | 250-290          | 240                                 | 250      | 292      |
| $+30^{\circ}/-30^{\circ}$     | 250-290          | 213                                 | 230      | 247      |
| $0^{\circ}_2/+30^{\circ}_2$   | 215-245          | 204                                 | 212      | 241      |
| $+30^{\circ}_2/-30^{\circ}_2$ | 215-245          | 153                                 | 162      | 169      |

## 6. Conclusions

An experimental investigation and FEM in angle-ply 2/2 twill weave T800 carbon/epoxy woven fabric composites laminates have been presented in this paper. Due to the high interlaminar normal and interlaminar shear stress gradients at the free-edge region, the inter-ply delamination represent as the main damage to allow final break. The static non-local criteria model (with and without gradient) have been proposed to predict the delamination onset and to overcome the mesh-dependence problems; Validation criteria was applied on the circular-hole specimens and shown a good prediction the position and stress of delamination onset.

## ACKNOWLEDGMENTS

We gratefully acknowledge ADEME (Agence de l'Environnement et de la Maîtrise de l'Energie) for

support from ARMINES Centre des Matériaux, in the project LICOS and ALSTOM.

## References

- [1] G. Nicoletto and E. Riva "Failure mechanisms in twill-weave laminates: FEM predictions vs. experiments" *Composites: Part A*, Vol. 35, pp. 787-795, 2004.
- [2] A.D. Kelkar, J.S Tate and R. Bolick "Structural integrity of aerospace textile composites under fatigue loading" *Material Science and Engineering B*, Vol. 132, pp. 79-84, 2006.
- [3] N. Alif, L.A. Carlsson and L. Boogh "The effect of weave pattern and crack propagation direction on mode I delamination resistance of woven glass and carbon composites" *Composites:Part B*, Vol. 29B, pp. 603-611, 1998
- [4] S.D. Pandita, G. Huvsmans, M. Wevers and I. Verpoest "Tensile fatigue behaviour of glass plain-weave fabric composites in on- and off-axis directions" *Composites: Part A*, Vol. 32, pp. 1533-1539, 2001
- [5] R.Y., Kim, and S.R. Soni, "Experimental and Analytical Studies on the onset of delamination in laminated composites", *Journal of Composites Materials*, Vol. 18, 1984, p. 71-80.
- [6] A. Diaz Diaz and J.F. Caron, "Prediction of the onset of mode III delamination in carbon-epoxy laminates", *Composite Structures*, Vol. 72, 2006, p. 438-445.
- [7] J.C. Brewer and P.A. Lagace, "Quadratic Stress Criterion for Initiation of delamination", *Journal of Composite Materials*, Vol. 22, 1988, p. 1141-1155.
- [8] L. Legunegrand, Th. Lorriot, R. Harry and H. Wargnier, "Design of an improved four point bending test on a sandwich beam for free edge delamination studies", *Composites: Part B* Vol. 37, 2006, p. 127-136.
- [9] Th. Lorriot, G. Marion, H. Harry and H. Wargnier, "Onset of free-edge delamination in composite laminates under tensile loading", *Composites:Part B*, Vol. 34, 2003, p. 459-471.
- [10] Z.P. Bažant and G. Pijaudier-Cabot, "Nonlocal continuum damage, localization instability and convergence", *Journal of Applied Mechanics*, Vol. 55, 1998, p. 287-293.N.
- [11] Germain, J. Besson, F. Feyel, and J.F. Maire, « Méthodes de calcul non local appliquées au calcul de structures composites », *Compiègne JNC14*, Vol. 2, 2005, p. 633-640.